J. Fluid Mech. (1980), *vol.* 99, *part* 1, *pp.* 129–144
Printed in Great Britain

A family of steady, translating vortex pairs with distributed vorticity

By R. T. PIERREHUMBERT

Department of Aeronautics and Astronautics, Massachusetts Institute of Technology, Cambridge, MA 02139

(Received 14 December 1978 and in revised form 1 October 1979)

An efficient relaxation method is developed for computing the properties of a family of vortex pairs with distributed vorticity, propagating without change of shape through a homogeneous, inviscid fluid. The numerical results indicate that a steady state exists even when the gap between vortices is arbitrarily small, and that as the gap closes the steady state approaches a limiting vortex pair with a cusp on the axis of symmetry. Comparison is made with an approximate theory due to Saffman, and agreement is found to be good until the vortices are almost touching. The energy of members of the family is computed, and possible means of experimental production are discussed.

1. Introduction

Norbury (1973) has constructed a family of vortex rings which vary continuously between a potential vortex and a Hill's spherical vortex, such that each vortex in the family consists of a core of constant potential vorticity embedded in irrotational fluid. The analogous problem in two dimensions, relating to a family of vortex pairs for which the vorticity itself is constant within the cores, has received little attention. While Norbury (1975) has proved that steady two-dimensional vortex pairs with vorticity confined to a compact region always exist provided that the vorticity is a Hölder continuous function of the stream function, the proof does not apply to the present case of uniform vortices, as the vorticity in this case is not even a continuous function of the stream function. Hence, it is of interest to see whether a family of uniform vortex pairs can be found, and to discover what happens as the gap between the vortices decreases. Deem & Zabusky (1978*a*, *b*, hereinafter referred to as DZ) have identified one member of such a family, which they refer to as a 'translating V-state', but have not exhibited the range of solutions possible, nor discussed their properties. In the present paper, we will present the results of a more detailed study of the two-dimensional problem. Specifically, we numerically calculate the steady-state shapes of a pair of simply connected, compact regions containing vorticity of opposite sign from each other, and embedded in irrotational fluid. The vorticity is assumed constant within each core. We restrict our discussion to solutions in which the boundary shapes have an axis of symmetry perpendicular to the direction of propagation, and in which the shapes are reflexions of each other about some line parallel to the direction of propagation. For each member of the family, propagation velocity, amount of entrained irrotational fluid, and kinetic energy are also determined. The energetic properties of the family are used to investigate the production of vortices by roll-up of the wake of a lifting surface, following on early work by Prandtl (1922) and Spreiter & Sacks (1951).

0022–1120/80/4469–1180 $02.00

The analytic calculation of the shape of a steady uniform vortex in a plane strain, performed by Moore & Saffman (1971), has been an invaluable theoretical tool in the study of two-dimensional vortices with finite-sized cores. One calculation based on this theory (Saffman 1979) predicts that a steady vortex pair with given cross-sectional area can be found regardless of how small the distance between vortex centroids is made, although the vortices become arbitrarily elongated as this distance decreases. It had remained unclear whether such solutions would continue to exist if the plane strain were replaced by the actual influence of the image vortex. This question is of particular importance because the existence of solutions for arbitrary closeness would indicate that a vortex pair could not disintegrate by mutually induced strain. It will be seen that, in the exact calculation, solutions continue to exist even when the gap between vortices is made arbitrarily small while holding the outer edges of the vortices fixed, but that the vortices approach a compact, limiting vortex pair in this limit rather than becoming indefinitely elongated, so that with fixed area the distance between centroids for compact steady vortices is bounded below. Nevertheless, we find that the approximate theory accurately predicts the propagation speed and degree of elongation of the numerically calculated vortex pair when the gap between vortex boundaries is as little as 10 % of the distance between centroids.

A major objective of this paper is to introduce a simple, efficient relaxation method for the solution of the one-dimensional nonlinear integral equation that appears in the problem. The method offers significant advantages over methods based on the Newton–Raphson iteration such as used by Norbury (1973) and DZ. Although certain information on the bifurcation properties of the equation is lost by using the relaxation method rather than Newton's method, there are many situations in which it is sufficient to find only one branch of the solution family, and in such circumstances the relaxation method presented here is an attractive alternative to Newton's method. The method generalizes easily to more complicated geometries than considered here; given the current level of interest in exploring steady configurations of vorticity in shear layers, jets, and wakes, we believe the relaxation method will find applications beyond the problem of propagating vortex pairs.

2. The governing equations

For the vorticity distribution described in the introduction the only criterion determining a steady solution is that the boundaries of the two regions containing vorticity be streamlines. Hence, if we can express the two-dimensional Stokes stream function, ψ, as a functional of the vortex boundary, the requirement that ψ be constant on the boundary immediately yields an integral equation for the boundary shape. This representation can be easily effected via the Green's function integral for the solution of Poisson's equation in two dimensions.

An example of the general type of vorticity distribution we will consider is shown in figure 1. Let $g(x)$ be the height of the boundary above the x axis, and assume the boundary shapes symmetrical about the x and y axes. We further stipulate

$$g(A_0) = g(A_1) = 0,$$

and $g > 0$ in between, with A_0 and A_1 positive. It is plausible that solutions with the assumed symmetry do exist, since the strain field induced by a vortex exhibits the

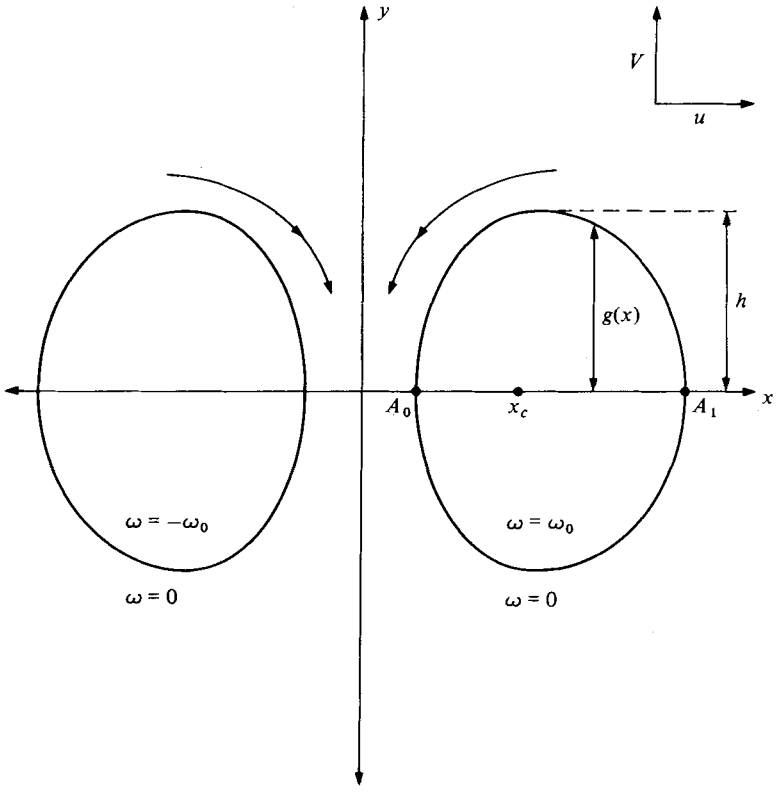

FIGURE 1. A core cross-section, with its defining characteristics. The boundaries that are shown separate regions of constant vorticity from irrotational fluid, and are assumed convex and symmetric about both the x and y axes. The parameter x_c is the centroid of the right-hand vortex, A_0 is the minimum distance from the y axis, and A_1 is the maximum distance from the y axis. The pair is propagating downward relative to fluid at rest at infinity.

same symmetries as the vortex itself. The parametrization of the boundary requires that any perpendicular to the x axis dropped from a point on the vortex boundary be entirely contained within the vortex. Hence there are certain possible non-convex solutions which are precluded by the present formulation of the problem. As will be seen in § 3, it is possible to identify a continuous family of vortices with the stated symmetry properties. The way in which other families of solutions enter the problem, for example through bifurcations from the symmetric family, is a separate problem of great theoretical interest. Let ω_0 be the absolute value of vorticity within the boundaries, and V_T the velocity of propagation, which points in the y direction. Then, in the reference frame moving with the vortex pair, the Green's function integral for the two-dimensional Poisson equation yields

$$\psi(x,y) = \frac{\omega_0}{2\pi}\int_{A_0}^{A_1}\int_{y=-g(x)}^{g(x)} \tfrac{1}{2}\log\left[(x-x')^2+(y-y')^2\right]dy'\,dx' - \frac{\omega_0}{2\pi}\int_{-A_1}^{A_0}\int_{-g(-x)}^{g(-x)} \tfrac{1}{2}\log\left[(x-x')^2+(y-y')^2\right]dy'\,dx' + V_T x. \quad (1)$$

The last term is added to satisfy the boundary condition of uniform flow at infinity.

The crucial simplification of these equations comes from the observation that, owing to the constant vorticity in the vortex cores, the integrals over y' in (1) can be evaluated analytically. It can easily be verified that

$$\int_{-g}^{g} \tfrac{1}{2}\log[(x-x')^2+(y-y')^2]\,dy' = -\left[(y-y')\left(\log[(x-x')^2+(y-y')^2]^{\frac{1}{2}}-1\right)+(x-x')\tan^{-1}\left(\frac{y-y'}{x-x'}\right)\right]\Bigg|_{y=-g(x)}^{y=g(x)}. \quad (2)$$

When this expression is substituted into (1) and the assumed symmetry properties are used, we are left with an expression for $\psi(x,y)$ in terms of the propagation velocity, V_T, and a one-dimensional integral involving $g(x)$. The resulting expression has the schematic form

$$\psi(x,y) = \psi_P(x,y)+V_T x, \quad (3a)$$

where

$$\psi_P(x,y) = \omega_0\int_{A_0}^{A_1} H_g(x,y|x')\,dx', \quad (3b)$$

and H_g depends on the function g, in accordance with (2). The integral equation for $g(x)$ now reads simply

$$\psi[x,g(x)] = c = \text{constant}. \quad (4)$$

We may non-dimensionalize the problem by defining the following quantities:

$$\left.\begin{aligned} \bar{x} &= x/A_1, & \bar{V}_T &= V_T/(\omega_0 A_1),\\ \bar{y} &= y/A_1, & \bar{c} &= c/(\omega_0 A_1^2),\\ \bar{H}_g &= H_g/A_1, & \bar{\psi} &= \psi/(\omega_0 A_1^2),\\ \bar{A}_0 &= A_0/A_1, & \bar{\psi}_P &= \psi_P/(\omega_0 A_1^2),\\ \bar{g} &= g/A_1. \end{aligned}\right\} \quad (5)$$

With these definitions, (4) becomes

$$\bar{c} = \int_{\bar{A}_0}^{1} \bar{H}_g(\bar{x},\bar{y}|\bar{x}')\,d\bar{x}' + \bar{V}_T\bar{x}. \quad (6)$$

Equation (6) appears to have three free parameters, namely $\bar{A}_0$, $\bar{V}_T$, and $\bar{c}$. However, from (6) and (3a) we observe that

$$\bar{\psi}(\bar{A}_0,0)-\bar{\psi}(1,0) = 0,$$

from which we easily find that

$$\bar{V}_T = \frac{\bar{\psi}_P(\bar{A}_0,0)-\bar{\psi}_P(1,0)}{1-\bar{A}_0}. \quad (7)$$

Then $\bar{c}$ is determined by

$$\bar{c} = \bar{\psi}_P(1,0)+\bar{V}_T. \quad (8)$$

Thus, for any curve $\bar{g}(\bar{x})$ there is a unique pair of values $(\bar{V}_T, \bar{c})$ for which $\bar{g}$ can possibly be a solution to (6). This implies that $\bar{V}_T$ and $\bar{c}$ are not free parameters, but instead must be determined simultaneously with the solution $\bar{g}$ to (6). The algorithm to be presented in the next section achieves this by computing $\bar{V}_T$ and $\bar{c}$ anew at each iteration using (7) and (8), thus ensuring that the solvability condition is always satisfied. $\bar{A}_0$, which emerges as the only free parameter of the problem, is held constant throughout the computation.

The present formulation of the problem differs from that of DZ in two respects. First, DZ represent the boundary as a general curve $(x(s), y(s))$, where s is the arc length along the curve. This difference is unimportant, as the integral in (6) can be trivially rewritten as a path integral along such a curve, computing dx' along the curve and using only the upper limit in (2) to find the kernel. In this manner boundary shapes as general as those examined by DZ can be treated within the present formulation. The second difference is that DZ express the steady-state condition in terms of the projection of velocity normal to the vortex boundary, whereas we use constancy of the stream function. We have chosen the latter formulation because it allows solution by the relaxation method to be described in § 3.

Substituting (8) for $\bar{c}$ into (6), we find that either the stream function or normal velocity formulation reduces to a nonlinear operator equation of the form

$$L(\partial S, \bar{V}_T, \bar{A}_0) = 0,$$

where ∂S is the vortex boundary. DZ specify $\bar{V}_T$ as the bifurcation parameter and essentially find $\bar{A}_0$ as a nonlinear eigenvalue, whereas we prefer to use $\bar{A}_0$ as the bifurcation parameter. The latter choice simplifies the numerical method, and provides somewhat better control over the kind of solution obtained.

3. Method of numerical solution

We will now describe a simple iterative procedure for solving (6)–(8) for $g(x)$. Henceforth, we will drop the bars over dimensionless quantities, except where it is necessary to distinguish them from dimensional quantities. The iteration begins with an initial guess $g^0(x)$. Once $g^N(x)$, the Nth iterate, is known, we can compute the vectors

$$\left.\begin{aligned} F_j^N &= \psi_P[x_j, g^N(x_j)] \\ G_j^N &= \partial_y \psi_P(x_j, y)|_{y=g^N(x_j)} \end{aligned}\right\} \quad \text{for} \quad j = 1, \ldots, M, \tag{9}$$

using (3 *b*). The vector $\{x_j\}$ represents a set of points on the x axis, between A_0 and A_1, which may have any desired spacing consistent with accurate representation of the boundary curve. The integrals required to evaluate F_j and G_j may be performed using any convenient numerical scheme; we used a trapezoidal integration scheme with a provision to subdivide the interval (x_j, x_{j+1}) when necessary to preserve accuracy of the integration. There is a logarithmic singularity in the integrand for G_j, but this may be dealt with in a straightforward fashion by analytically calculating the contribution from the singular part of the integrand.

Next, we compute an estimate of V_T using equation (7), which is

$$V_T^N = \frac{F_1^N - F_M^N}{1 - A_0}, \tag{10}$$

and also compute the estimate

$$c^N = F_M^N + V_T^N. \tag{11}$$

Now we define a vector of residues

$$R_j^N = (F_j^N + V_T^N x_j) - c^N, \tag{12}$$

which, by definition, vanishes when g satisfies the system of integral equations. Hence, we want to adjust $g(x_j)$ at each iteration so as to reduce the magnitude of the vector R_j.

This can be done by Newton's method, as used by Norbury for the case of vortex rings and DZ for V-states. However, implementing Newton's method for this system requires the solution of a linear integral equation at each iteration. In the discrete approximation, this requires the evaluation, storage, and inversion of an $M \times M$ matrix, the elements of which must usually be computed numerically. This involves storage of $O(M^2)$ and an operation count of $O(M^3)$. Clearly, if the need to evaluate and invert this matrix could be circumvented, considerable savings in computer time per iteration and in programming effort would result. Motivated by these observations, we have developed a relaxation scheme that offers improvements in simplicity over Newton's method, and requires overall storage of only $O(M)$ and an operation count of $O(M^2)$ per iteration. We can only offer a heuristic justification of the method, but experience with the problem at hand indicates that convergence to a solution is always obtained.

The justification for our method is that, since V_T^N, c^N, and ψ_P are all related to g^N by integral expressions, they should be relatively insensitive to small changes in g^N, and hence most of the change in R_j will come from the fact that we are computing ψ_P at a different point, rather than the fact that we are changing the shape of the boundary. With this assumption, if we write

$$\hat{g}(x_j) = g^N(x_j) + \Delta_j,$$

then the change in F_j is given by

$$\begin{aligned}\hat{F}_j &\cong \psi_P(x_j, g^N(x_j) + \Delta_j) \\ &\cong \psi_P(x_j, g^N(x_j)) + \left(\frac{\partial \psi_P(x_j, y)}{\partial y}\bigg|_{y=g^N(x_j)} \right) \Delta_j \\ &\cong F_j^N + G_j^N \Delta_j,\end{aligned}$$

where ψ_P is computed using g^N as the boundary curve. Since Δ_j vanishes at the boundary points $j = 1$ and $j = M$, the change in V_T and c due to the increment of g may be neglected. Hence, substituting into the expression for the residual vector,

$$\hat{R}_j \cong R_j^N + \Delta_j G_j^N.$$

As the estimate for the increment, we therefore take

$$\Delta_j = -R_j^N / G_j^N. \tag{13}$$

With this formula we can increment g and begin the process over again, starting with (9). However, since the estimate of Δ_j given by (13) is reliable only if Δ_j is small, we can only take (13) as giving an estimate of the direction in increment space by which to change $\{g(x_j)\}$ in order to reduce the residual. Therefore, at the risk of slowing convergence for the sake of ensuring stability, we multiply Δ_j by an under-relaxation factor K before incrementing, so that the incrementation rule is

$$g^{N+1}(x_j) = g^N(x_j) + K\Delta_j, \quad 0 < K < 1. \tag{14}$$

The iteration is completed and the next iteration is begun by using g^{N+1} as the new estimate. A value of $K = 0{\cdot}6$ was found to ensure convergence in all cases encountered.

The advantages of the relaxation algorithm over Newton's method come at a price, however. The $M \times M$ matrix computed in implementing Newton's method is an approximation to the Frechet derivative with respect to $g(x)$ of the nonlinear operator

given by the right-hand side of (6). Except for isolated members of the solution family, the Frechet derivative will be invertible. Those points at which the Frechet derivative is not invertible represent possible bifurcation points of the system. Modern developments in bifurcation theory have shown how to use the kernel and cokernel of the derivative at bifurcation points to continue the solution onto the several branches that can emanate from the bifurcation point. (This theory is well covered in Berger (1977), especially pp. 154–158, 163–192, and 272–277.) This is an indisputably attractive feature of Newton's method, and the speed and simplicity of the relaxation method must be weighed against the loss of this bifurcation information in deciding which method to use. It should be kept in mind, though, that in many cases the primary bifurcation is from a simple flow, for which bifurcation information may be obtained analytically. This is the case for bifurcation from a parallel shear layer into a family of shear-layer vortices, as treated by Pierrehumbert & Widnall (1979) and Saffman & Szeto (1979), and also for bifurcation from a circular vortex into families of uniformly rotating V-states, as treated by DZ. Information on secondary bifurcation points is harder to obtain without Newton's method, but we note that neither Saffman & Szeto nor DZ needed to make use of this information to perform their calculations.

4. Discussion of numerical results

The calculations outlined above were carried out with M points spaced according to the formula

$$x_j = \tfrac{1}{2}(A_0+A_1)+\tfrac{1}{2}(A_0-A_1)\cos\left((j-1)\pi/(M-1)\right)$$

so as to provide more resolution in the regions where the boundary becomes vertical. Calculations were initially performed with $M = 50$, and truncation error was estimated by checking the results for representative vortices in the family against runs with $M = 80$. A further check was provided by comparing the values for the smaller, essentially circular vortices against readily available analytical results. All numerical values presented should be accurate to the number of significant figures stated. The relaxation algorithm was found to have first-order convergence properties, with $\|\Delta g^N\| \leqslant \epsilon \|\Delta g^{N-1}\|$ asymptotically in the maximum norm; for $K = 0{\cdot}6$, ϵ was conservatively estimated as $0{\cdot}5$ from experience with the algorithm. In accordance with the first-order convergence properties, a fixed accuracy δ in $g(x)$ was obtained by accepting convergence when $\|\Delta g\| \leqslant \frac{1}{2}\delta$. For most calculations we set

$$\delta = \tfrac{2}{3}(A_1-A_0)/(M-1)$$

because this choice resulted in at least two decimal place accuracy in the vortex properties when $M = 50$ and allows for refinement of the values when M is increased. The convergence of Newton's method is second order (Berger 1977, pp. 116–118) and therefore requires far fewer iterations than relaxation for a specified level of convergence. It can be seen very simply that in most cases the lower operation count of relaxation more than offsets the convergence rate of Newton's method. Let N_1 be the number of relaxation iterations needed to reduce the initial error by a factor $\delta/\Delta g^0$, and N_2 the equivalent number for Newton's method. Then first-order convergence implies $N_1 = \ln(\delta/\Delta g^0)/\ln\epsilon$ whereas second-order convergence implies

$$N_2 = \ln\left[\ln(\delta/\Delta g^0)/\ln\epsilon\right]/\ln 2.$$

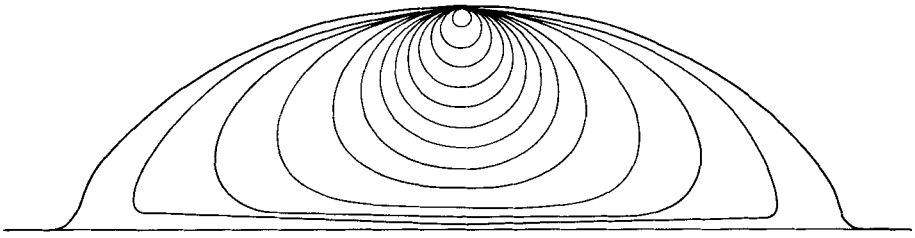

FIGURE 2. The family of solutions to the steady vortex pair problem. The displayed curves represent boundaries between rotational and irrotational flow for various members of the family. The image vortices are not shown, as they are merely the reflexions of these curves about the horizontal axis. In this figure the outer edge of the vortex is held fixed for all members and the gap between the vortices is varied. Values of R/x_c for the curves, from outside in, are: 2·16, 1·97, 1·55, 1·22, 0·844, 0·639, 0·500, 0·390, 0·225, 0·159, 0·100 and 0·048.

If ϵ is about the same for the two methods, the ratio of operation count for relaxation to reach convergence to that for Newton's method is approximately

$$n = N_1/(MN_2) = N_1 \ln 2/(M \ln N_1),$$

using M^2 operation count for relaxation and M^3 for Newton's method. In computing the family of vortices we began with circular vortices at $\bar{A}_0$ close to unity, and progressed to smaller $\bar{A}_0$ using a similarity scaling of the previously computed vortex as an initial guess for the next vortex boundary. With steps in $\bar{A}_0$ on the order of 0·1 each new vortex required under six iterations for convergence to the previously stated level of accuracy. With $M = 50$ and $N_1 = 6$ we then have $n = 0{\cdot}05$, so that relaxation saves an estimated factor of twenty in computer time over Newton's method. Of course, if N_1 were to increase indefinitely with M fixed, Newton's method would eventually win out, but there is little point in increasing the convergence accuracy without also increasing M, as $N_1 = 6$ already yields accuracy comparable to truncation error (due to trapezoidal integration) over most of the boundary. In any event, the break-even point for $M = 50$ does not occur until $N_1 \simeq 600$, at which point the initial error is reduced by a factor of 10^{-180}, representing a number of significant figures enormously beyond the number likely to be required in any calculation of this type. These figures are subject to some change, depending on programming details and the true value of ϵ for Newton's method, but the direction of the advantage is clear. It is notoriously difficult to predict actual timing for a given machine, but as a rough guide we found that each relaxation iteration with $M = 50$ takes 1·5 seconds on a Texas Instruments ASC, using scalar code. The timing is $O(M^2)$ for scalar code, and can be reduced to $O(M)$ for vector code, since the integrals needed in the relaxation method can all be done in parallel. It was not necessary to use vector code, as the net computation time was not great enough to make the additional programming effort worth while. The speed of the algorithm even in scalar form makes it ideal in cases where available computer resources are limited.

The family of boundary curves satisfying (6) is shown in figure 2. In this figure, A_1 (the co-ordinate of the outer edge of the region containing vorticity) is held fixed while A_0 (the co-ordinate of the inner edge) is varied from a small positive value to a value close to A_1. The quantity $\bar{A}_0 = A_0/A_1$ provides a non-dimensional measure of the gap between vortices. As would be expected, the vortex boundary becomes circular for

$\bar{A}_0$ near unity and becomes highly distorted when $\bar{A}_0$ is small. We have taken the calculation to $\bar{A}_0 = 0{\cdot}001$ and always found a steady solution. The vortex does not become indefinitely elongated as $\bar{A}_0 \to 0$, but instead approaches a limiting shape. Through a minor modification of our program it was possible to set $\bar{A}_0 = 0$ and calculate the limiting vortex directly. This vortex is shown together with the others in figure 2. In the region $x < 0{\cdot}1A_1$ the limiting vortex boundary becomes rapidly steeper as the y axis is approached, although this region is too small to accurately resolve in figure 2. The steepening was confirmed by running the algorithm to a convergence level of a tenth the customary level, so that the slopes could be accurately computed. This property of the boundary suggests that the actual solution has a cusp on the y axis. By considering the flow field near the point of contact between the right-hand vortex and the y axis it can be shown that this is indeed true.

Consider the point of contact between the right-hand vortex boundary and the negative-y axis, and let r be the distance from this point and θ the angle around this point, with $\theta = 0$ pointing along the negative-y axis. Then, if the contact angle is θ_0, the stream function in the vicinity of the point is determined in the region $0 \leqslant \theta \leqslant \pi$ by

$$\left.\begin{aligned} \nabla^2\psi_{\mathrm{I}} &= 0 \quad \text{for} \quad \theta < \theta_0, \\ \psi_{\mathrm{I}}(r, 0) &= \psi_{\mathrm{I}}(r, \theta_0) = 0, \end{aligned}\right\} \tag{15}$$

and

$$\left.\begin{aligned} \nabla^2\psi_{\mathrm{II}} &= -\omega_0 \quad \text{for} \quad \theta > \theta_0, \\ \psi_{\mathrm{II}}(r, \pi) &= \psi_{\mathrm{II}}(r, \theta_0) = 0. \end{aligned}\right\} \tag{16}$$

Also, we must require continuity of the tangential velocity across the line $\theta = \theta_0$, that is,

$$\left.\frac{\partial\psi_{\mathrm{I}}}{\partial\theta}\right|_{\theta_0} = \left.\frac{\partial\psi_{\mathrm{II}}}{\partial\theta}\right|_{\theta_0}. \tag{17}$$

The case $\theta_0 = \frac{1}{2}\pi$ is immediately precluded, since the boundary conditions for (16) imply that $\psi_{xx} = \psi_{yy} = 0$ at the corner, and hence the vorticity must also vanish at the corner, implying that no continuous solution can exist in the region containing vorticity. As for the general case, it may readily be verified that

$$\psi_{\mathrm{II}} = \frac{\omega_0 r^2}{4}\left(\frac{\cos(2\theta - \theta_0)}{\cos\theta_0} - 1\right) \tag{18}$$

and

$$\psi_{\mathrm{I}} = Br^{\alpha}\sin\alpha\theta, \tag{19}$$

where $\alpha = \pi/\theta_0$. Substituting in (17), we find

$$B\alpha r^{\alpha} = \tfrac{1}{4}\omega_0 r^2 \tan\theta_0. \tag{20}$$

Obviously, equation (20) cannot be satisfied for non-zero θ_0, regardless of the choice of B. Hence we conclude that the slope ($\cot(\theta_0)$) of the vortex boundary must become infinite where it joins the axis, implying the existence of a cusp.

Moore & Saffman (1971) have shown that the steady-state shape of a uniform vortex in a plane strain is elliptical, and that a steady elliptical state can exist only when the strain rate relative to the core vorticity is sufficiently small. Saffman (1979) has used their result to estimate the properties of a vortex pair with distributed vorticity, such as has been considered in the present work. The results of the approximate calculation are in agreement with our numerical results in that a steady state exists for $\bar{A}_0$

arbitrarily small. However, the approximate elliptical vortices become elongated to an arbitrarily great extent in this limit, whereas the actual solutions do not. This discrepancy arises because c (the value of the stream function on the vortex boundary) must approach zero as $\bar{A}_0$ becomes small, so that the vortex boundary must become identical with the separating streamline $\psi = 0$ in this limit, and the portion of the vortex boundary nearest the y axis must approach the y axis. An elliptical vortex cannot satisfy this requirement without becoming indefinitely elongated, whereas the inner portion of the true vortex boundary is free to become vertical without affecting the outer portion. It is possible that the family we have exhibited can be continued past the limiting vortex into a family for which the region containing vorticity is not compact, but extends to infinity along the y axis; we have made no attempts to find such vortices.

In order to facilitate quantitative comparison between the numerical and approximate results, we have evaluated a number of non-dimensional characteristics of the numerically determined vortex pair. We first define the centroid of the right-hand vortex

$$x_c = \frac{\int_{A_0}^{A_1} x\, g(x)\, dx}{\int_{A_0}^{A_1} g(x)\, dx}, \tag{21}$$

which is a dimensional measure of the closeness of the vortices. The area of the same vortex is obviously given by

$$S = 2\int_{A_0}^{A_1} g(x)\, dx, \tag{22}$$

whence the circulation $\Gamma = \omega_0 S$ is found. A measure of the vortex size is the effective radius R, given by

$$R = (S/\pi)^{\frac{1}{2}}. \tag{23}$$

This is the radius the vortex would have if it were circular. A convenient non-dimensional parametrization of the vortex family is then R/x_c. When $R/x_c \gg 1$, the vortex size is large compared to its distance from the image vortex, and so will be considerably distorted. A useful velocity scale is

$$V_0 = \Gamma/(4\pi x_c), \tag{24}$$

which is the propagation velocity the vortex pair would have if all the vorticity were concentrated in point vortices at $x = \pm x_c$. The corresponding non-dimensional propagation velocity is $V_T^* = V_T/V_0$. As a non-dimensional measure of the distortion of the vortex we take the maximum vortex height relative to the vortex half-width, $h/[\frac{1}{2}(A_1 - A_0)]$, which approaches unity for nearly circular vortices. As before, we use A_0/A_1 as the non-dimensional measure of the distance of closest approach of the vortices. The non-dimensional quantities we have defined are similar to those used by Saffman. These and other characteristics of the vortices shown in figure 2 are given in table 1.

In figure 3 we have plotted the aforementioned vortex characteristics as functions of R/x_c, along with the approximate results due to Saffman. From this figure it is

R/x_c	x_c/A_1	A_0/A_1	$2h/(A_1-A_0)$	V_T^*	c/Γ	y_s/x_c	x_s/x_c	$Q/(2S)$	T^*
0·048	0·955	0·9091	1·00	1·00	−0·51	1·73	2·09	719	0·63
0·100	0·909	0·8182	1·01	1·00	−0·40	1·73	2·09	180	0·52
0·159	0·864	0·7273	1·01	1·00	−0·32	1·73	2·09	71·6	0·45
0·225	0·818	0·6364	1·03	1·00	−0·27	1·73	2·09	35·7	0·39
0·390	0·726	0·4545	1·08	1·00	−0·18	1·74	2·09	11·9	0·30
0·500	0·679	0·3636	1·13	0·99	−0·14	1·75	2·09	7·36	0·26
0·639	0·631	0·2727	1·22	0·98	−0·11	1·78	2·09	4·58	0·22
0·844	0·577	0·1818	1·40	0·94	−0·067	1·87	2·11	2·79	0·18
1·22	0·510	0·09091	1·82	0·83	−0·028	2·20	2·17	1·64	0·13
1·55	0·469	0·04545	2·27	0·72	−0·012	2·68	2·24	1·26	0·098
1·97	0·429	0·009091	2·94	0·59	−0·0018	3·53	2·35	1·05	0·073
2·16	0·4130	0	3·41	0·54	0	4·13	2·42	1·00	0·064

TABLE 1. Table of vortex properties. S is the area of one vortex, $R = (S/\pi)^{\frac{1}{2}}$; A_0, A_1, and h are defined in figure 1; x_c is the centroid of the right-hand vortex; V_T^* is the normalized translation velocity; c is the value of stream function on the vortex boundary; Γ is the circulation of right-hand vortex; y_s is the y intercept of the separating streamline; x_s is the x intercept of the separating streamline; Q is the total cross-sectional area enclosed by the separating streamline; T^* is the normalized kinetic energy.

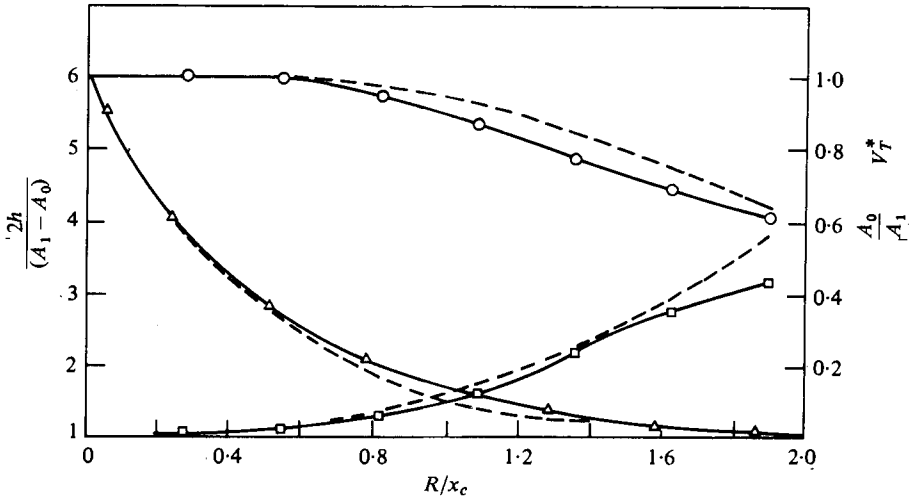

FIGURE 3. Properties of the family of vortex pairs. R/x_c parametrizes the family. When it is small the vortices approximate point vortices and when it is large the vortices are nearly touching (see text for details). -○-○-○-, normalized translation velocity, V_T^*; -□-□-□-, vortex elongation, $2h/(A_1-A_0)$; -△-△-△-, normalized intervortex gap, A_0/A_1. Broken lines indicate the approximate results of Saffman.

evident that the approximate results agree quite well with the more precise numerical results, even when R/x_c is as large as 1·9, the only appreciable divergence appearing in the values for elongation when the vortices are close. The greater elongation predicted by the approximate theory arises partly because the exact shape of the vortex boundary is skewed toward the line of symmetry, as shown in figure 2, whereas the approximate vortex shape is symmetric about the line $x = x_c$, which coincides with its major axis. Given identical vortex area and distortion, this asymmetry makes x_c smaller for the

exact solution, and hence R/x_c larger. At fixed R/x_c, then, the distortion is expected to be less for the numerical solution. The divergence is most pronounced when the vortices are close, as the asymmetry is most pronounced in this case. The overestimate of elongation in the approximate theory when the vortices are close also reflects the fact that the exact solutions approach a limiting vortex, whereas the approximate solutions do not.

The decrease in V_T^* from its asymptotic value of unity is quantitatively similar for the numerical and approximate calculations, and in either case may be traced to the elongation of the vortices as they approach each other. Essentially, when all the vorticity is concentrated in a small region, the velocity induced at a given point on a vortex by its image receives nearly the same contribution from each point on the image. When the vortices are elongated, however, the contributions from the distant portions of the image vortex are significantly less than those from the near portions, and the total induced velocity is correspondingly less than if the same circulation were concentrated in a smaller region.

Once the vortex boundaries have been found, it is an easy matter to compute the properties associated with the vortex pairs, such as the separating streamline and kinetic energy. We have found that up to $R/x_c = 0{\cdot}85$ the separating streamline is very like that for a pair of point vortices located at $\pm x_c$. (This curve may be found in Batchelor (1967).) As R/x_c is increased past this point, the separating streamline approaches the vortex boundary, until the two become identical at the limiting vortex. In table 1 we have given the y intercept, y_s, and the x intercept, x_s, of the separatrix in units of x_c. We have also given the cross-sectional area Q of the lens of fluid carried along with the vortex pair, in terms of the total vortex area $2S$. The energetic properties are discussed in § 5.

5. Energetic constraints on the production of vortex pairs by roll-up

In this section we consider the possibility of producing the vortex pairs we have computed by the two-dimensional roll-up of a vortex sheet such as might be shed into the wake of a wing. The results presented here must be interpreted in the light of two caveats. First, roll-up of a vortex sheet probably will not result in uniform vortices, so the results may be taken only as a crude estimate of the size of vortices produced. Second, the assumption of two-dimensional roll-up is not a very good one for highly swept or low aspect-ratio wings, for which roll-up is rapid and three-dimensional effects are bound to be important. In the latter case leading-edge separation can further complicate the situation.

Consider an initial state consisting of a vortex sheet on the x axis between $x = -b$ and $x = b$, having circulation per unit length $\gamma(x) = -\gamma(-x)$. Such a vortex sheet could be produced in the wake of a wing having bound circulation distribution $\Gamma(x)$ defined by $\gamma(x) = -d\Gamma/dx$. Note that the magnitude of total circulation shed into each trailing vortex is $\Gamma_0 = \Gamma(0)$. We now consider the constraints placed on the final state produced by inviscid roll-up, owing to the conservation of impulse, energy, and Γ_0. Pioneering work along these lines was done by Prandtl (1922) and Spreiter & Sacks (1951) for the case of circular vortices; our contribution is to extend the calculation to the case where the final state is not circular.

One of the conserved quantities can be eliminated by dimensional analysis, and we take it to be Γ_0. If T is the total kinetic energy of the vortex pair computed in the reference frame where the fluid is at rest at infinity, P the Kelvin impulse, and ρ the fluid density, we can define non-dimensional energy and impulse as $T^* = T/(\rho\Gamma_0^2)$ and $P^* = P/(\rho b\Gamma_0)$. (Precisely speaking, T and P are energy and impulse per unit length in the z direction.) Spreiter & Sacks recognized that P^* is proportional to x_c/b, where x_c is the centroid of vorticity as defined earlier, so that x_c for the initial and final states are the same. This would not be the case if mutual destruction of vorticity by viscous diffusion were allowed. For uniform vortices, T^* can be conveniently computed in terms of a path integral along the vortex boundary, as we have discussed elsewhere (Pierrehumbert & Widnall 1979). The values of T^* for the family of vortex pairs are given in table 1. The quantity x_c for the initial vortex sheet determines x_c for the vortex pair, thus setting the fundamental length scale. It is T^* that determines which member of the family is selected.

Ashley & Landahl (1965) have given a formula for computing the T^* of a wing-wake. If θ is defined by $x = b\sin\theta$ and $\Gamma(x)$ is represented by a Fourier series

$$\Gamma(x) = 2\sum_{j=1}^{\infty} B_j \cos((2j-1)\theta), \tag{25}$$

then their formula can be cast in the form

$$T^* = \frac{\pi}{8}\frac{\sum_{j=1}^{\infty}(2j-1)B_j^2}{\left(\sum_{j=1}^{\infty}B_j\right)^2}. \tag{26}$$

From (25) it is easily found that

$$\frac{x_c}{b} = \frac{\pi}{4}\frac{B_1}{\sum_{j=1}^{\infty}B_j}. \tag{27}$$

For an elliptically loaded wing $B_1 = 1$ and $B_j = 0$ for $j > 1$, so $T^* = \pi/8 \simeq 0{\cdot}39$. Thus, referring to table 1 an elliptically loaded wing will produce trailing vortices with $R/x_c = 0{\cdot}225$. This is in close agreement with the value of 0·192 found by Spreiter & Sacks. The difference arises because Spreiter & Sacks computed the energy of the vortex pair under the assumption $R/x_c \ll 1$, and when R/x_c is as large as 0·2 some of the neglected terms are not truly insignificant, even for circular vortices. We have found that when these terms are included the calculation based on circular vortices yields the same result as the numerical calculation, as it should, since the vortices are still essentially circular at $R/x_c = 0{\cdot}225$. The variable T^* is a monotonic decreasing function of R/x_c, so to produce distorted vortices we must find leading distributions with lower T^*.

In fact, T^* for the initial state can be made arbitrarily small. If we take

$$B_j = 1/(2j-1) \quad \text{for} \quad j \leqslant N \quad \text{and} \quad B_j = 0 \quad \text{for} \quad j > N$$

we find from (26) that

$$T_N^* = \frac{\pi}{8}\frac{1}{\sum_{j=1}^{N}(2j-1)^{-1}}. \tag{28}$$

x	$\phi_{66}(x)$	x	$\phi_{66}(x)$
0	1·0000	0·2007	0·3780
0·002625	0·9951	0·2198	0·3523
0·005469	0·9793	0·2404	0·3448
0·008550	0·9509	0·2626	0·3249
0·01189	0·9097	0·2864	0·3149
0·01551	0·8569	0·3121	0·2944
0·01943	0·7962	0·3397	0·2868
0·02367	0·7338	0·3692	0·2675
0·02828	0·6776	0·4008	0·2517
0·03326	0·6353	0·4334	0·2409
0·03866	0·6115	0·4703	0·2280
0·04451	0·6041	0·5082	0·2133
0·05085	0·6035	0·5483	0·1985
0·05771	0·5956	0·5903	0·1839
0·06515	0·5712	0·6340	0·1680
0·07320	0·5349	0·6793	0·1506
0·08192	0·5046	0·7255	0·1378
0·09136	0·4940	0·7722	0·1216
0·1016	0·4925	0·8184	0·1075
0·1126	0·4753	0·8631	0·08939
0·1246	0·4439	0·9048	0·07255
0·1376	0·4286	0·9418	0·05558
0·1516	0·4258	0·9719	0·03905
0·1667	0·4021	0·9924	0·02083
0·1831	0·3821	1·0000	0

TABLE 2. Normalized load distribution to produce a vortex with $T^* = 0{\cdot}13$. b is the semispan and the distribution is symmetric in x; $x_c/b = 0{\cdot}064$ for this distribution.

Also, $x_c/b = \frac{1}{2}T^*$ in this case. The corresponding bound circulation distribution, normalized so $\Gamma_0 = 1$, will be called $\phi_N(x/b)$. The integral test immediately demonstrates that the denominator in (28) grows without bound as N is increased, and becomes logarithmically infinite for large N. The functions ϕ_N for moderate to large N fall off rapidly from unity while x/b is small, and thereafter decrease more gradually to zero as $x/b \to 1$. The function ϕ_{66}, corresponding to $T^* = 0{\cdot}13$, is given in table 2. This loading distribution corresponds to a moderately distorted vortex pair with $R/x_c = 1{\cdot}22$. Since $x_c/b = 0{\cdot}064$ for this distribution, the vortices are small compared to the span and lie close to the centre of the wing. From table 2 it is evident that a wing with such a loading distribution would have to have a highly swept leading edge, and under such circumstances leading-edge separation would be likely to occur, and the assumptions used to predict T^* would become invalid. Though a more sophisticated theory would be needed to treat this case, the energy comparison indicates that only wings with very steep leading edges are likely to produce vortices that are appreciably distorted. We note that, if the induced drag D_i is measured directly in an experiment, R/x_c for the wake is determined by $T^* = D_i/(\rho\Gamma_0^2)$, regardless of the conditions under which roll-up occurs.

6. Conclusions

We have exhibited a continuous family of vortex pairs with uniform vorticity, ranging from a pair of pointlike vortices to a limiting vortex pair in which the vortex

boundaries are in contact along the axis of symmetry and have a cusp on that axis. The existence of a limiting vortex, and consequently of an upper bound for R/x_c for compact steady vortices, stands in contrast to the approximate results of Saffman (1979), which indicated that a steady state could be found for arbitrarily large R/x_c. Nevertheless, the approximate theory accurately predicts a number of vortex characteristics even when it is operating well outside the rigorous range of validity discussed by its originator. By examining the energy of the vortex pairs, we have concluded that vortices deviating appreciably from circularity are unlikely to be produced in the wakes of wings of practical interest. We have, however, described a family of lift distributions corresponding to planforms with highly swept leading edges, which have some potential for producing the more distorted vortices described in this paper.

Under most circumstances the relaxation method developed for computing the vortex family will perform considerably better than Newton's method in terms of number of operations needed to achieve convergence, although information on the location of secondary bifurcation points is lost by using the relaxation method. By virtue of its simplicity, our method is easy to extend to other geometries. We have already used the algorithm to construct the steady states of periodic arrays of uniform vortices in a shear layer (Pierrehumbert & Widnall 1979).† It is likely that relaxation would also be useful in investigating the structure of vortex streets and uniformly rotating vortices.

The author wishes to express gratitude to the Knox Foundation, which provided support while he was a research student at the Department of Applied Mathematics and Theoretical Physics, Cambridge, where the work herein presented was begun. The author is also indebted to N. O. Weiss (D.A.M.T.P.) and S. E. Widnall (M.I.T.) for many valuable discussions. This work was made possible by the generous provision of computer time by the N.O.A.A. Geophysical Fluid Dynamics Laboratory, Princeton, N.J. This research was partially supported by the National Science Foundation under contract number 7414978-ENG.

† Saffman & Szeto (personal communication, 1979) approached this problem simultaneously and independently using Newton's method and arrived at solutions virtually identical with ours.

REFERENCES

ASHLEY, H. & LANDAHL, M. 1965 *Aerodynamics of Wings and Bodies*, pp. 135–137. Addison-Wesley.

BATCHELOR, G. K. 1967 *An Introduction to Fluid Dynamics*, p. 534. Cambridge University Press.

BERGER, M. S. 1977 *Nonlinearity and Functional Analysis*. Academic.

DEEM, G. S. & ZABUSKY, N. 1978*a* Stationary 'V-states', interactions recurrence, and breaking. In *Solitons in Action* (eds K. Longren & A. Scott), pp. 277–293. Academic.

DEEM, G. S. & ZABUSKY, N. 1978*b* Stationary 'V-states', interactions, recurrence and breaking. *Phys. Rev. Lett.* **40**, 859–862.

MOORE, D. W. & SAFFMAN, P. G. 1971 Structure of a line vortex in an imposed strain. In *Aircraft Wake Turbulence* (ed. J. H. Olsen, A. Goldburg & M. Rogers), pp. 339–353. Plenum.

NORBURY, J. 1973 A family of steady vortex rings. *J. Fluid Mech.* **57**, 417–431.

NORBURY, J. 1975 Steady planar vortex pairs in an ideal fluid. *Comm. Pure Appl. Math.* **28**, 679–685.

PIERREHUMBERT, R. T. & WIDNALL, S. E. 1979 The structure of organized vortices in a free shear layer. *A.I.A.A. Paper* 79-1560.

PRANDTL, L. 1922 Über die Entstehung von Wirbeln in der Idealen Flüssigkeit. In *Gesammelte Abhandlungen*, pp. 697–714. Springer.

SAFFMAN, P. G. 1979 The approach of a vortex pair to a plane surface in inviscid fluid. *J. Fluid Mech.* **92**, 497–503.

SPREITER, J. R. & SACKS, A. H. 1951 The rolling up of the trailing vortex sheet and its effect on downwash behind wings. *J. Aero. Sci.* **18**, 21–32.